Supplementary Information

Polyoxometalate-Encapsulated Metal-Organic Framework for Photocatalytic Uranium Isolation

Zhimin Dong[#], Dongling Zeng[#], Zifan Li, Junjie Chen, Youqun Wang, Xiaohong Cao, Guoping Yang*, Zhibin Zhang*, Yunhai Liu, Feng Yang*

Results and Discussion

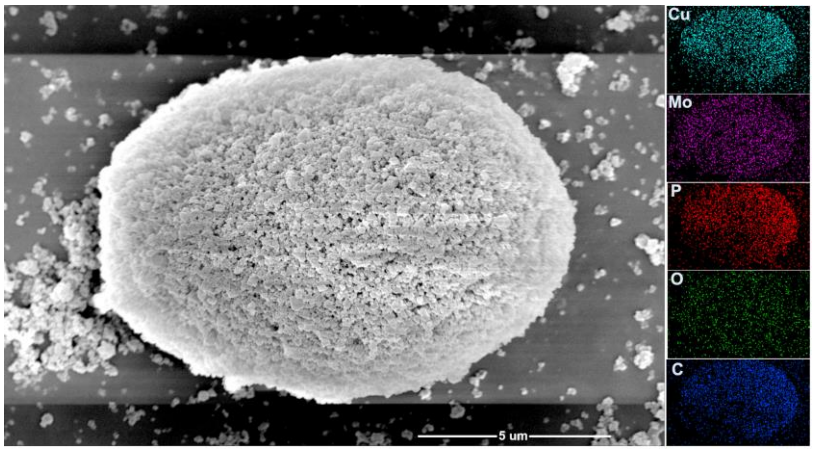

Figure S1. SEM image and EDS mapping of POM@Cu-MOFs.

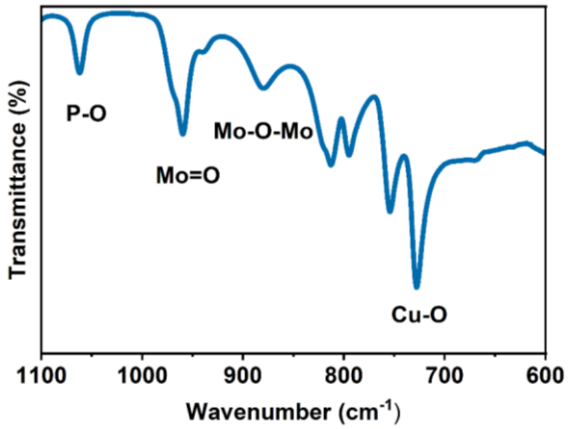

Figure S2. Partially magnified FT-IR spectrum of POM@Cu-MOFs at 600 to 1100 cm^{-1}.

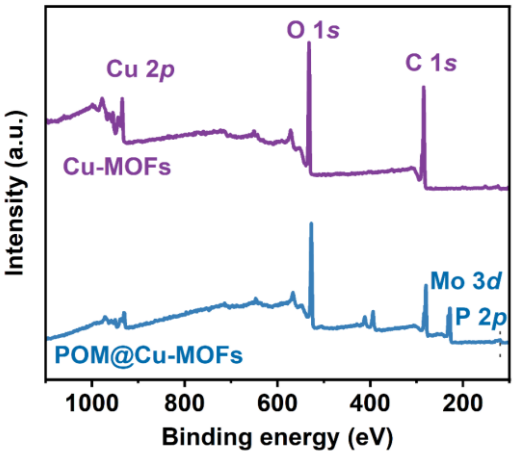

Figure S3. The survey scan of XPS spectra of Cu-MOFs and POM@Cu-MOFs.

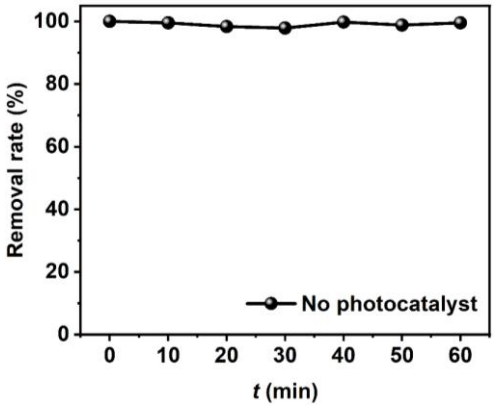

Figure S4. Removal performance of U(VI) without photocatalyst ($C_{U(VI)}$ = 50 mg·L^{-1}, *pH* = 4.0, C_{Ca2+} = 0.001 mol·L^{-1}).

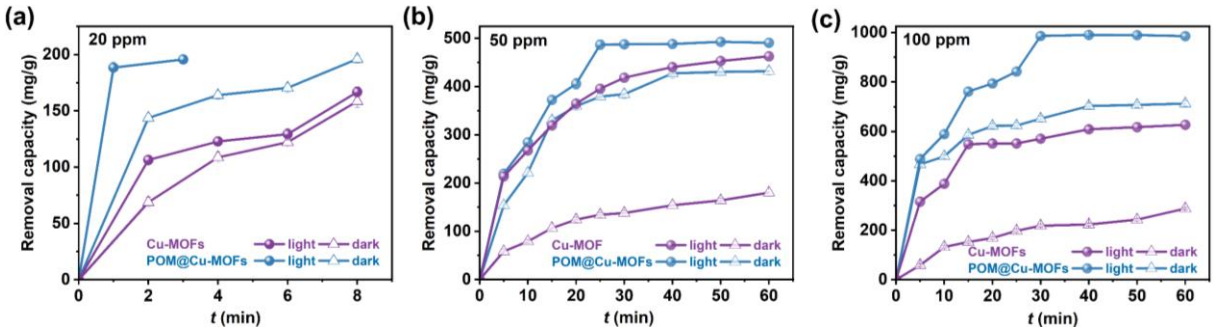

Figure S5. Uranium removal by Cu-MOFs and POM@Cu-MOFs using the photocatalytic reduction method compared to the adsorption method in the dark with initial uranium concentrations of (a) ~20 mg·L^{-1}, (b) ~50 mg·L^{-1}, (c) ~100 mg·L^{-1} (*m*/*V* = 0.1 g·L^{-1}, *pH* = 4.0, C_{Ca2+} = 0.001 mol·L^{-1}).

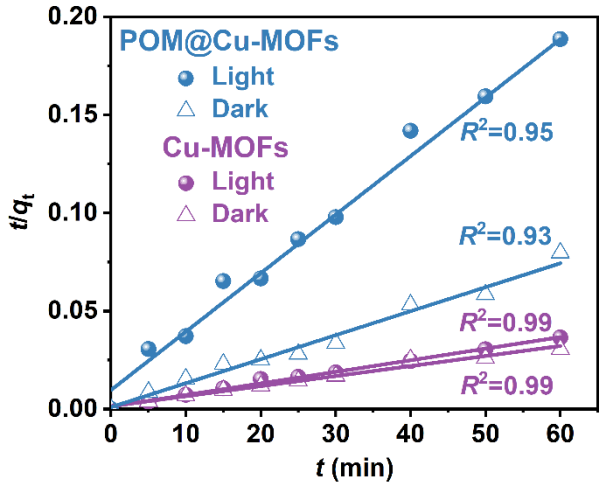

Figure S6. The pseudo-second-order kinetics model for Cu-MOFs and POM@Cu-MOFs photocatalytic isolation of U(VI) with an initial uranium concentrations of ~200 mg·L^{-1}.

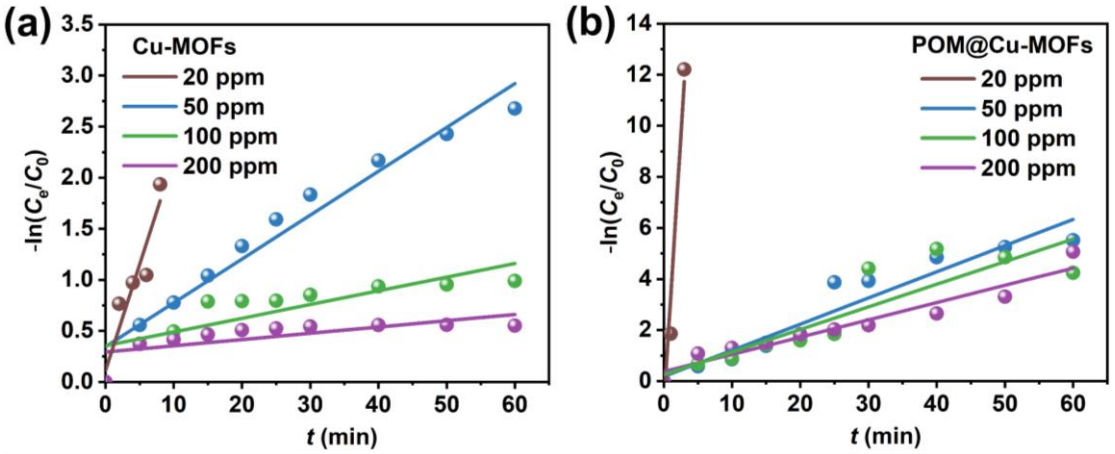

Figure S7. Corresponding pseudo-first-order kinetics model for photocatalytic isolation of U(VI) with different concentrations over (a) Cu-MOF and (b) POM@Cu-MOF catalysts.

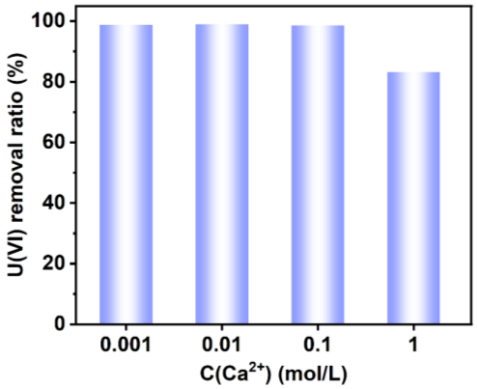

Figure S8. Effect of Ca^{2+} concentration on photocatalytic removal of uranium ($C_{U(VI)}$ = 50 mg·L^{-1}, m/V = 0.1 g·L^{-1}, pH = 4.0).

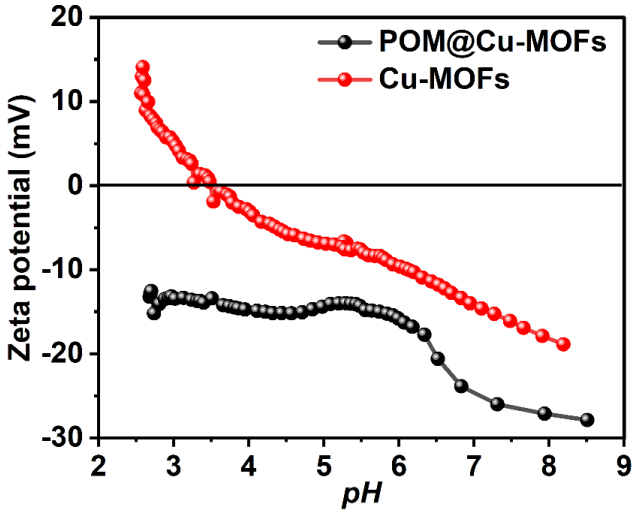

Figure S9. Surface zeta potentials of Cu-MOFs and POM@Cu-MOFs.

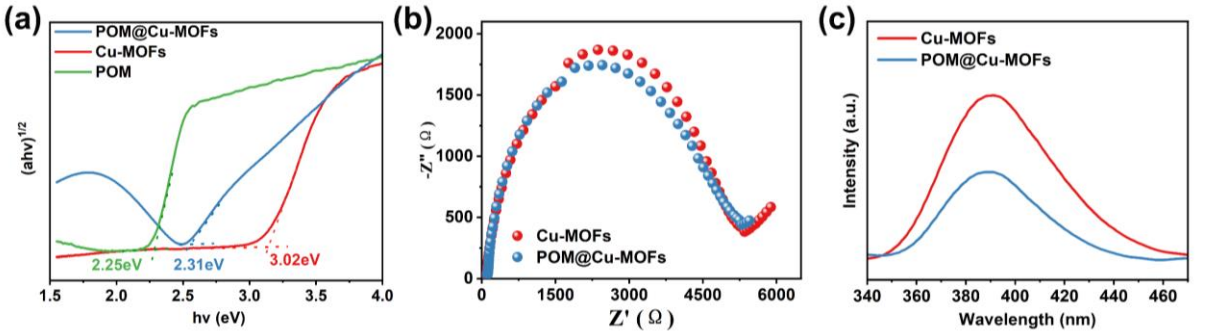

Figure S10. (a) Plots of transformed Kubelka-Munk function versus photon energy. (b) Electrochemical impedance spectroscopy Nyquist plots of Cu-MOFs and POM@Cu-MOFs. (c) PL spectroscopy of Cu-MOFs and Cu-MOF@POM.

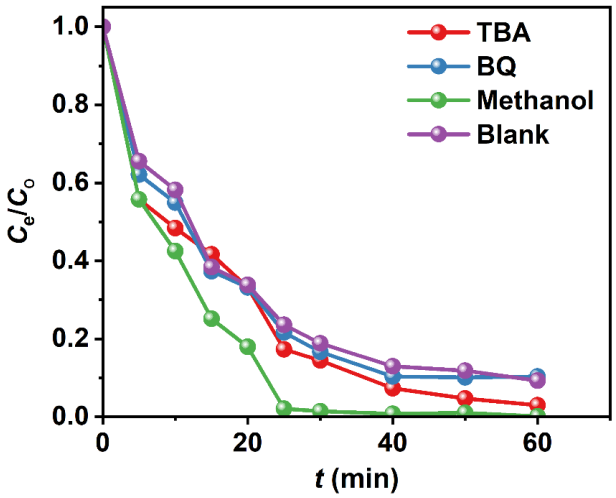

Figure S11. Effect of radical quenching on phenol degradation with POM@Cu-MOFs.

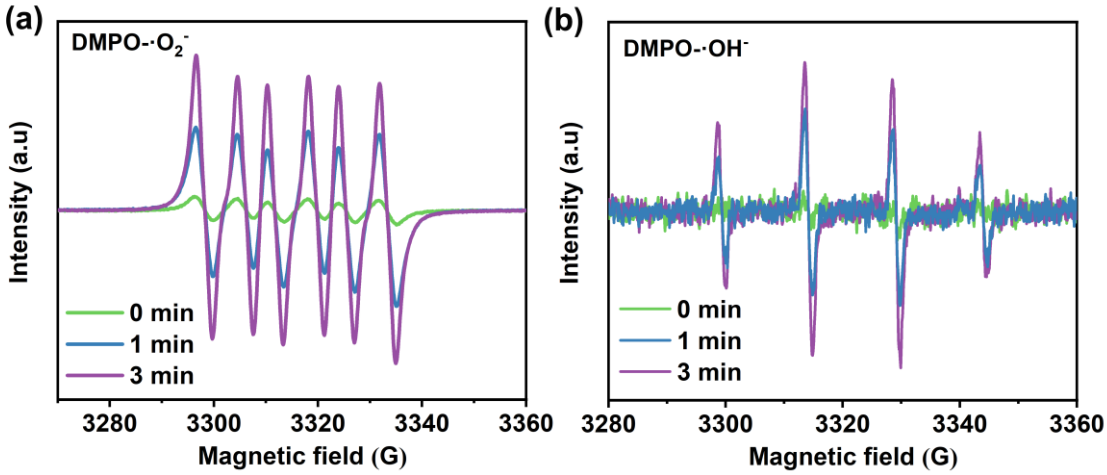

Figure S12. ESR signals of (a)·O_2^- and (b)·OH in the POM@Cu-MOFs before and after illumination.

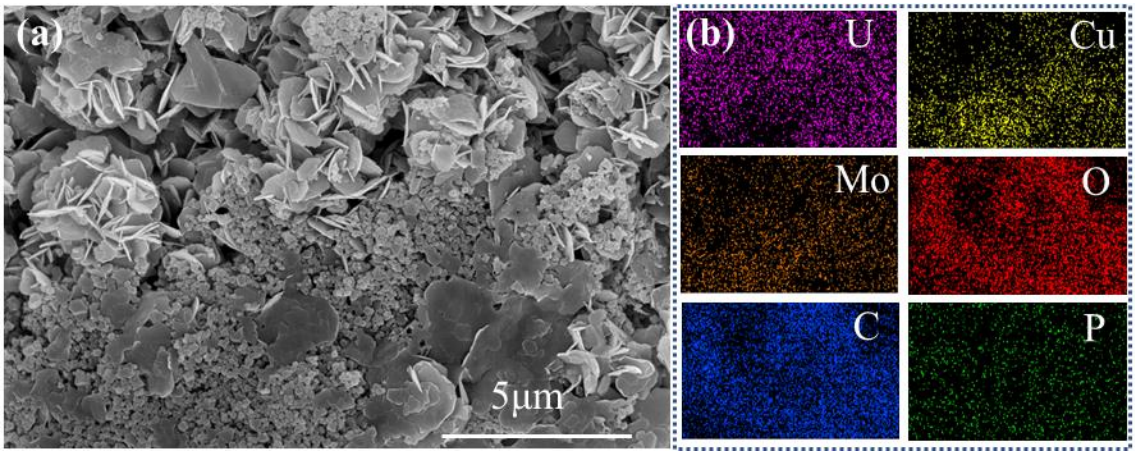

Figure S13. SEM image of POM@Cu-MOFs after photocatalytic reduction (a) and EDS mapping (b).

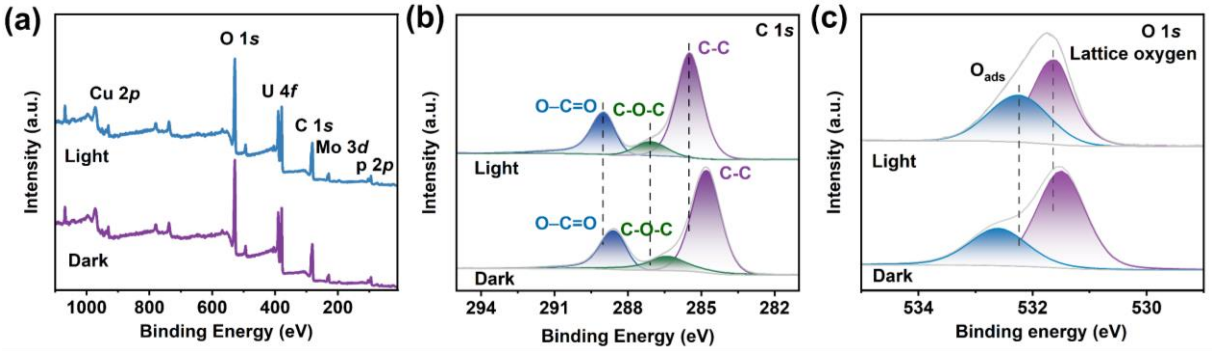

Figure S14. Comparison of the XPS spectra of POM@Cu-MOFs after photocatalytic reduction and absorption: (a) survey spectra, (b) C 1*s*, and (c) O 1*s*.

Table S1. Comparison of adsorption capacity of various materials for U(VI) ions

Sorbents	Condition	pH	m/V (g/L)	C_0 (mg·L^{-1})	q_e (mg/g)	Ref.
PMo_{12}/UiO-66	Photocatalysis	5.5	0.2	160	225.36	[S1]
SCU-19	Photocatalysis	4	0.5	400	728.34	[S2]
PN-PCN-222	Photocatalysis	4	0.25	400	1289.3	[S3]
Bi_2WO_6	Photocatalysis	6.5	0.057	30	246.75	[S4]
GO-POM	Adsorption	4	0.2	50	232.04	[S5]
CS-NZVI	Adsorption	5	0.1	30.94	591.72	[S6]
POM@Cu-MOFs	Photocatalysis	4	0.1	200	1637.39	This work

Supplemental reference

S1. Z. Zhang, Z. Li, Z. Dong, F. Yu, Y. Wang, Y. Wang, X. Cao, Y. Liu, and Y. Liu, *Chin. Chem. Lett*., 2022, **33**, 3577–3580.

S2. H. Zhang,, W. Liu, A. Li,, D. Zhang, X. Li,, F. Zhai, L. Chen,, L. Chen,, Y. Wang, S. Wang, *Angew. Chem. Int. Ed*., 2019, **58**, 16110–16114.

S3. H. Li, F. Zhai, D. Gui, X. Wang, C. Wu, D. Zhang, X. Dai, H. Deng, X. Su, J. Diwu, *Appl. Catal. B Environ. Energy,* 2019, **254**, 47–54.

S4. X. Zhong, Y. Liu, T. Hou, Y. Zhu, B. Hu, *J. Environ. Chem. Eng*., 2022, **10**, 107170.

S5. X. Han, Y. Wang, X. Cao, Y. Dai, Y. Liu, Z. Dong, Z. Zhang, Y. Liu, *Appl. Surf. Sci*., 2019, **484**, 1035–1040.

S6. Q. Zhang, D. Zhao, S. Feng, Y. Wang, J. Jin, A. Alsaedi, T. Hayat, C. Chen, *J. Colloid Interface Sci*., 2019, **552**, 735–743.